An integrated approach for classifying the cloudy boundary layer

Marke[1], T., S. Crewell[1], U. Löhnert[1], J. Schween[1], A. J. Manninen[2], E. J. O'Connor[2], and U. Rascher[3]

[1] Institute of Geophysics and Meteorology, University of Cologne, [2] Finnish Meteorological Institute, Helsinki, [3] Research Center Jülich

1. Introduction to the Measurement Site JOYCE

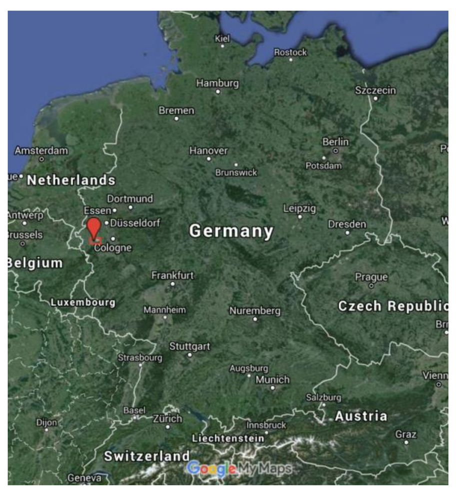

***Fig. 1:** Location of the JOYCE site in Jülich, Germany.*

***Fig. 2:** JOYCE Instruments (left to right): Doppler Lidar, Microwave Radiometer, Ceilometer, Cloud Radar,120 m Meteorological Tower and Eddy Covariance station*

Continuous and temporally highly-resolved measurements of the **cloudy boundary layer** are provided at the Jülich Observatory for Cloud Evolution (**JOYCE**, Fig. 1) since 2011, by using ground based passive and active remote sensing and in-situ instruments (Fig. 2).

2. Site Characterization with Ground Based Observations

- Macro-physical properties of boundary layer clouds are assessed with the synergy of a ceilometer and cloud radar.
  - ➢ High monthly variability of the **total cloud cover** (Fig. 3)

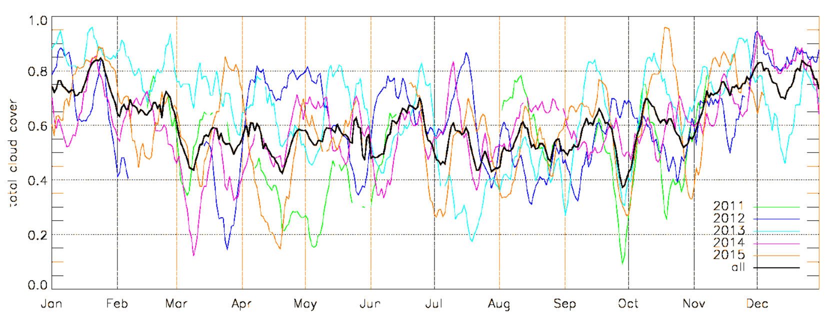

***Fig. 3:** 10 day center moving average of Ceilometer daily mean total cloud cover for JOYCE.*

- Comparison of remote sensing and in-situ derived **wind direction** to a weather type classification model (Fig. 4)
  - ➢ Influences of the local and synoptic scale can be identified.

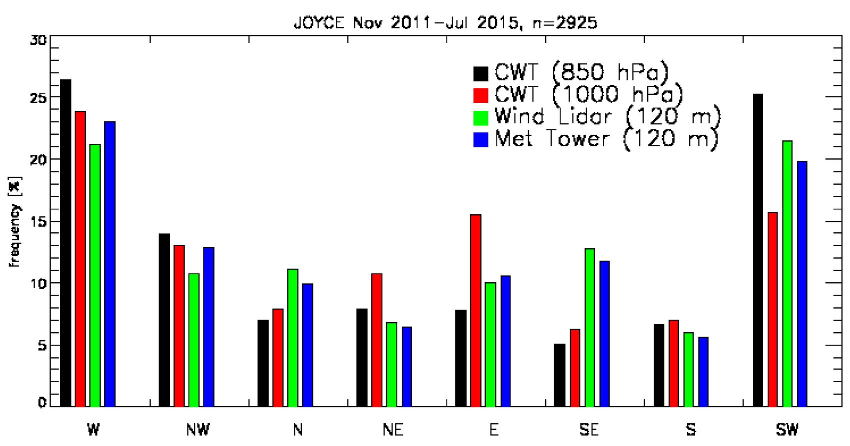

***Fig. 4:** Wind direction derived from Doppler Lidar and Meteorological Tower (120 m) and Circulation Weather Type Classification based on ERA-Interim 850 hPa / 1000 hPa.*

- **Azimuth scans** using a microwave radiometer (Fig. 5) provide the spatial distribution and gradient of the **integrated water vapor (IWV)**.
  - ➢ Link to exchange processes of the surface.

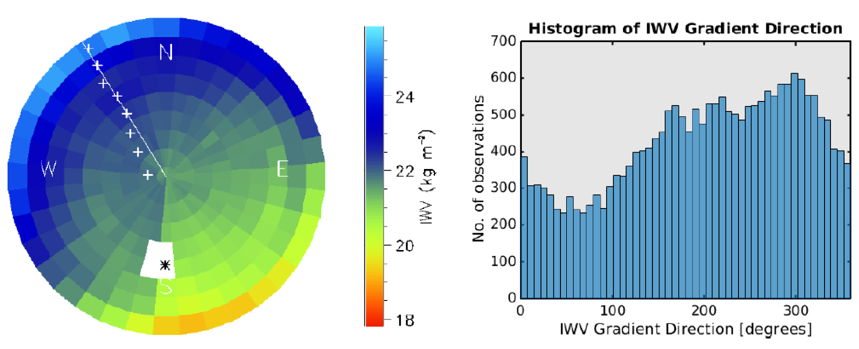

***Fig. 5:** Left: Air mass corrected IWV field and IWV gradient derived from one microwave radiometer hemispheric scan. Right: IWV gradient direction histogram.*

3. Link to Surface Patterns and Model Evaluation

- **HyPlant**: high-resolution airborne imaging spectrometer for vegetation monitoring (sun-induced and chlorophyll **fluorescence**, Fig. 6)
  - ➢ Link between IWV scans and surface patterns

***Fig. 6:** HyPlant fluorescence imager (670-780 nm) with a 3 m resolution*

- **ICON** (ICOsahedral Nonhydrostatic): unified modeling system for global numerical weather prediction (NWP) and climate studies that performs as a **large eddy simulation (LES)** model (Fig. 7)
  - ➢ Evaluate BL type parameterizations

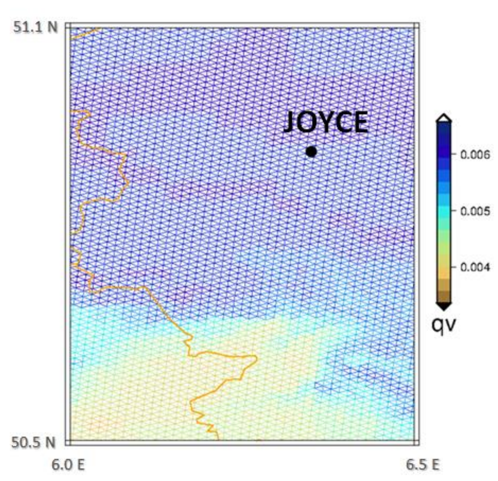

***Fig. 7:** Water vapor mixing ratio qv (kg/kg) from a ICON model run at around 800 m height with a 624 m horizontal resolution*

4. A Scheme to Classify the Cloudy Boundary Layer

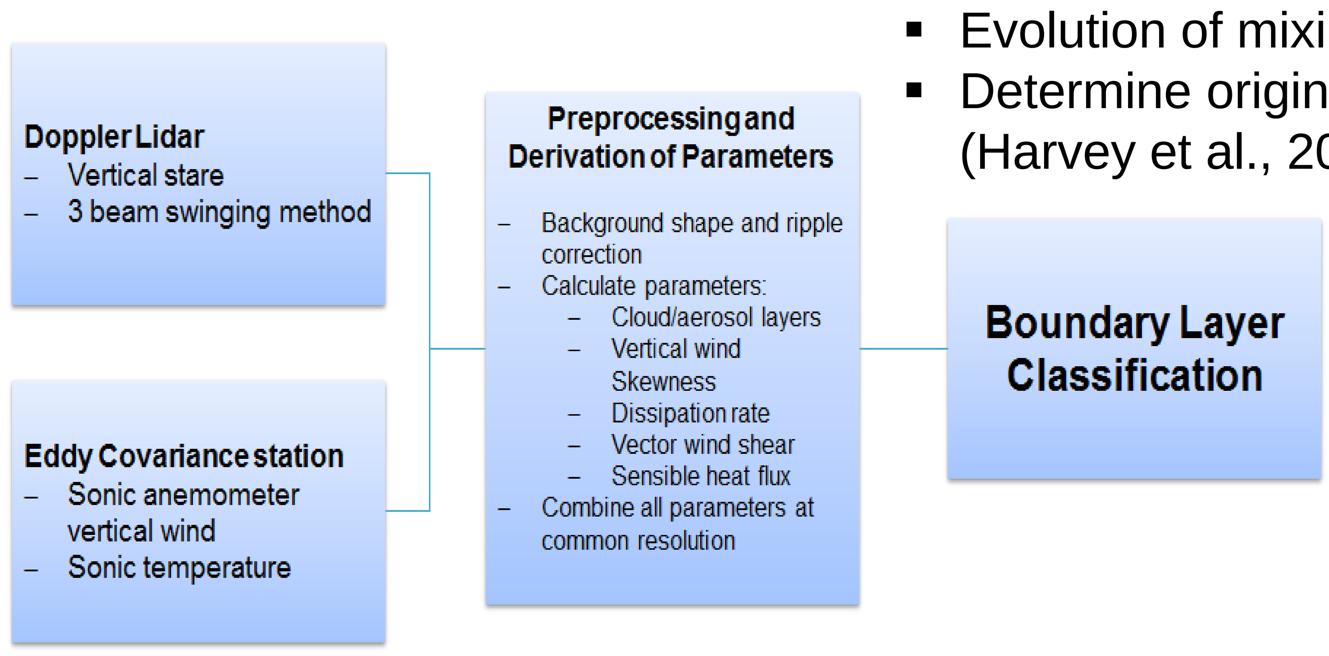

***Fig. 8:** Schematic representation of the boundary layer classification.*

- Evolution of mixing processes
- Determine origin of turbulence (Harvey et al., 2013)

Preprocessing of Doppler Lidar Data

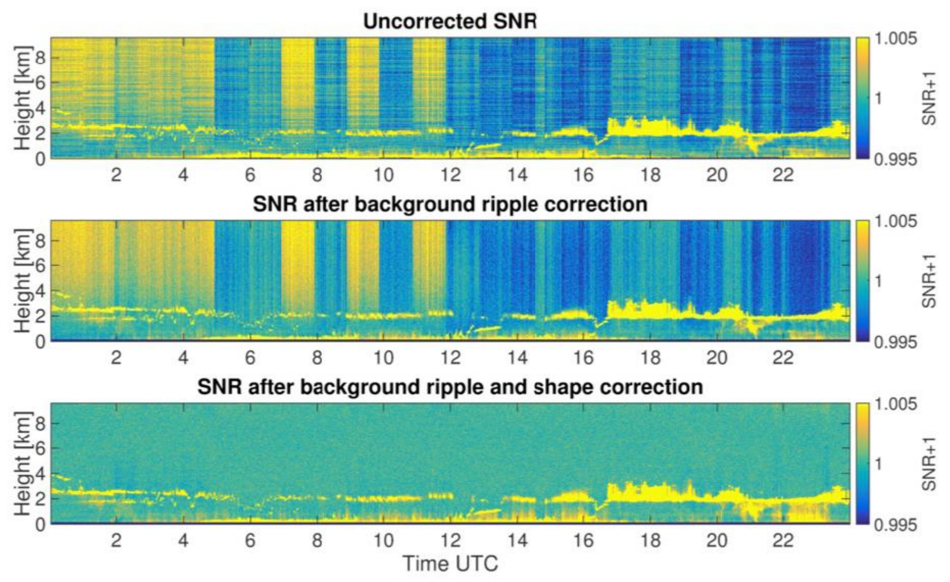

***Fig. 9:** Doppler lidar SNR before and after correction.*

Background shape correction (Manninen et al., 2015) and ripple correction (Vakkari et al., to submit)

- ➢ Homogeneous background
- ➢ Allows lower signal-to-noise ratio (SNR) threshold
- ➢ Bias in turbulent properties is reduced

Observations and Derived Parameters

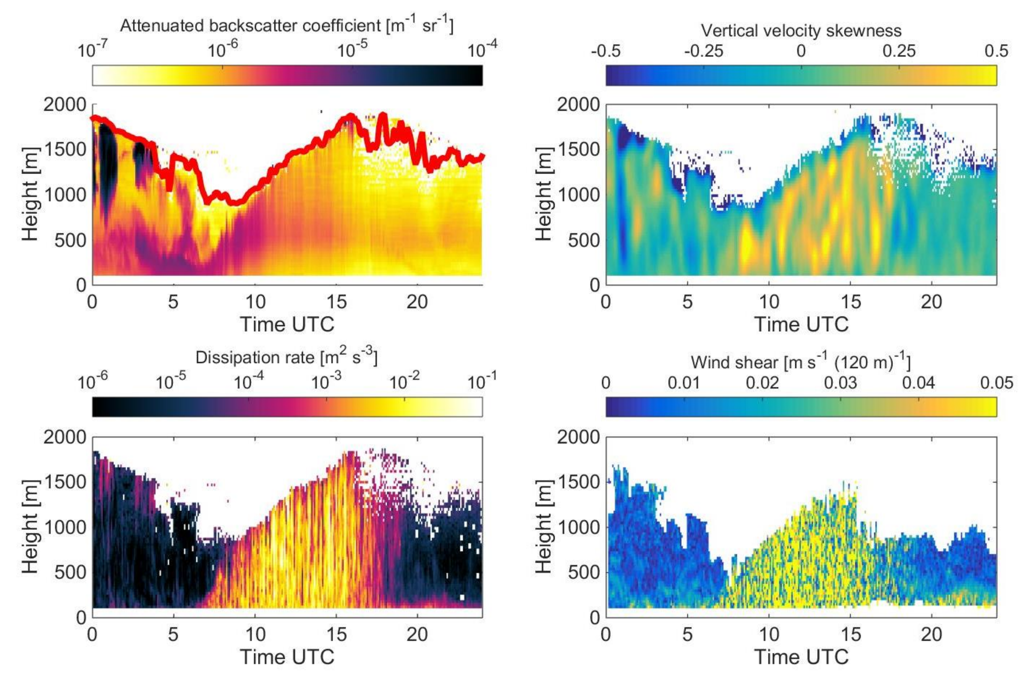

***Fig. 10:** Time series of the attanuated backscatter coefficient, vertical velocity skewness, dissipation rate and vector wind shear (clockwise from top left).*

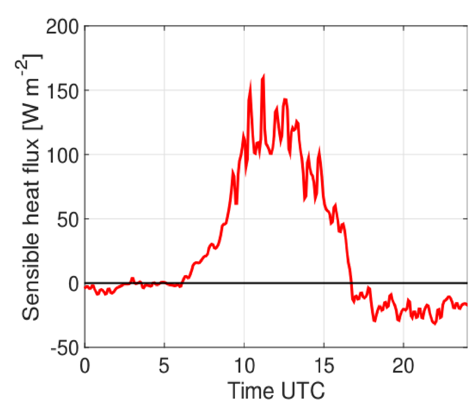

***Fig. 11:** Time series of the sensible heat flux derived from the EC station.*

5. Boundary Layer Classification Results

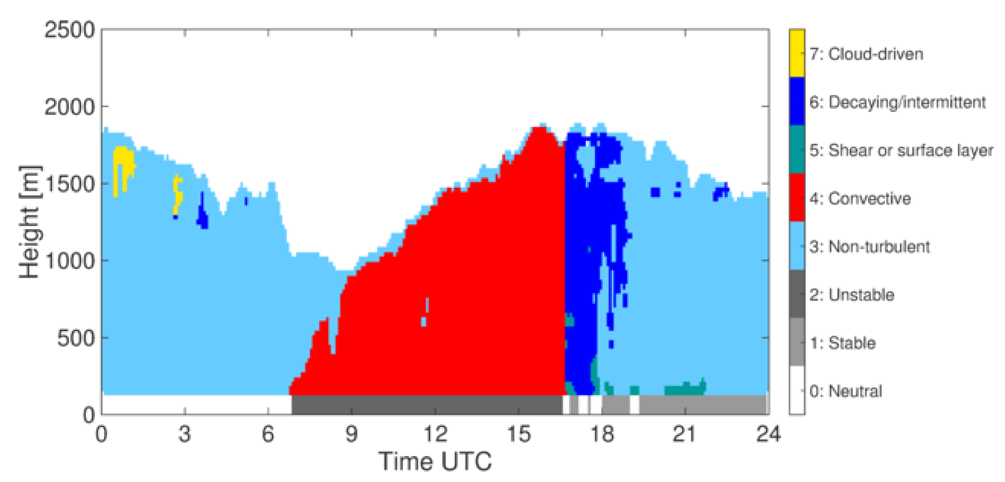

***Fig. 12:** Illustration of the bit-field, showing the boundary layer classification.*

- Each pixel in the common resolution grid (temporal: 5 min, vertical: 30 m) is classified using a **bit-field**.
- Type decisions are based on **threshold** values (Table 1)

Parameter	Attenuated backscatter coefficient	Vertical velocity skewness	Dissipation rate	Vector wind shear	Sensible heat flux
Threshold	10^{-5}	0	10^{-4} m^2 s^{-3} 10^{-3} m^2 s^{-3}	0.02 m s^{-1} per 100 m	0 W m^{-2} ±10 W m^{-2}

***Table 1:** Thresholds used for the bit-field.*

Outlook: Operational use in the **Cloudnet** (Illingworth et al., 2007) framework.

References:

Dipankar, A., B. Stevens, R. Heinze, C. Moseley, G. Zängl, M. Giorgetta, and S. Brdar, 2015: Large eddy simulation using the general circulation model ICON, J. Adv. Model. Earth Syst., 7, 963-986.

Harvey, N. J., R. J. Hogan, and H. F. Dacre, 2013: A method to diagnose boundary-layer type using Doppler lidar, Q. J.R. Meteorol. Soc., 139, 1681-1693.

Illingworth, A. J., and Coauthors, 2007: Cloudnet: Continuous evaluation of cloud profiles in seven operational models using ground-based observations. Bull. Amer. Meteor. Soc., 88, 883-898.

Manninen, A. J., E. J. O'Connor, V. Vakkari, and T. Petäjä, 2015: A generalised background correction algorithm for a Halo Doppler lidar and its application to data from Finland, Atmos. Meas. Tech. Discuss., 8, 11139-11170.

tmarke@meteo.uni-koeln.de